

## Laboratory-Frame View of Nuclear Rotation

Takaharu Otsuka

*Department of Physics, University of Tokyo, Hongo, Bunkyo-ku, Tokyo, 113, Japan  
and Institute for Nuclear Theory, University of Washington, Seattle, Washington 98105  
(Received 18 March 1993)*

A novel interpretation of nuclear rotation is presented. It is shown that, in and near the ground state, the proton and neutron deformed ellipsoids are rotating in opposite directions, whereas they rotate about almost the same axis in states of higher spins. This holds, quite similarly, for angular-momentum-projected Nilsson wave functions and for wave functions in the interacting boson model. The rotational energy can then be interpreted in terms of an inertial parameter against tilting of the proton rotation axis towards the neutron axis.

PACS numbers: 21.60.Ev, 21.10.Re, 21.60.Fw

Rotational motion is the most prominent mode in nuclear structure, and it appears in a large number of nuclei. In this Letter, we shall discuss the rotational motion in the ground-state (rotational) band of even-even nuclei with relatively low rotational frequency. The intuitive picture of such low-frequency nuclear rotation is that the nucleus is deformed in an ellipsoidal shape, and this ellipsoid rotates about an axis. We shall restrict ourselves to axially symmetric prolate deformation where the above rotation occurs about a shorter axis. The nuclear many-body system consists of protons and neutrons. We therefore introduce the proton ellipsoid and the neutron ellipsoid, which correspond, in the Nilsson model, to the proton intrinsic state and the neutron intrinsic state, respectively [1,2]. In the interacting boson model (IBM) [3], a separation of proton-neutron degrees of freedom is also present in its proton-neutron version, IBM-2 [4-6]. In this Letter, we shall study the rotation of the proton ellipsoid and that of the neutron ellipsoid in terms of the Nilsson model and the IBM-2. As stated in most textbooks of nuclear physics, it has been supposed rather *a priori* that the proton ellipsoid and the neutron ellipsoid rotate together in ground-state rotational bands. We will be led to a rather novel picture of the rotation as we shall see in the following.

We start with the Nilsson model [1,2], where nucleons are confined in a quadrupole deformed potential (Nilsson potential), and a pairing interaction acts between either protons or neutrons. The proton intrinsic state,  $|\Phi_\pi\rangle$ , is written in the form of the BCS ground state in terms of the canonical single-particle basis states of the Nilsson potential. The neutron intrinsic state,  $|\Phi_\nu\rangle$ , is determined similarly. The subscripts  $\pi$  or  $\nu$  indicate, respectively, protons or neutrons. The total Nilsson wave function is given by their product,  $|\Psi\rangle = |\Phi_\pi\rangle \times |\Phi_\nu\rangle$ , and describes the structure of rotational nuclei. This product relation is found in some other mean field theories, for instance, Hartree-Fock-Bogoliubov (HFB). The proton or neutron Nilsson wave function is given as

$$|\Phi\rangle \propto P_N \prod_{m>0} (u_m + v_m a_m^\dagger a_{\bar{m}}^\dagger) |0\rangle, \quad (1)$$

where the subscript  $\pi$  or  $\nu$  is omitted for brevity,  $u$  and  $v$

denote the BCS  $u$  and  $v$  factors,  $m$  represents the canonical single-particle basis with  $\bar{m}$  being its time-reversed state, and  $a_m^\dagger$  stands for the nucleon creation operator. Formula (1) contains the particle number projector  $P_N$ , because the number-conserving BCS/HFB code based on the method of Ref. [7] is used.

The Nilsson wave function is obtained with a deformed potential, and hence does not have a good angular momentum. By projecting the Nilsson wave function onto components with good angular momenta, one obtains members of a rotational band, the ground-state band in the present study. We then carry out the projection onto a good total angular momentum  $J$ . We consider the axially symmetric deformation with  $K^P = 0^+$ ; the actual calculation is performed by the standard method of integration over the Euler angle  $\beta$ , where matrix elements of a scalar operator  $\hat{O}$  are given by

$$\langle J | \hat{O} | J \rangle = \frac{\int_0^\pi d\beta \sin\beta d_{00}^J(\beta) \langle \Psi | \hat{O} \exp(-i\beta \hat{J}_y) | \Psi \rangle}{\int_0^\pi d\beta \sin\beta d_{00}^J(\beta) \langle \Psi | \exp(-i\beta \hat{J}_y) | \Psi \rangle}, \quad (2)$$

where  $\hat{J}_y$  is the  $y$  component of the total angular momentum operator  $\mathbf{J}$ , and  $d_{00}^J$  denotes a  $d$  function.

We show the result for  $^{156}\text{Sm}$  as an example. The deformation parameter is taken as  $\delta = 0.30$ , and the monopole pairing interaction is set with the pairing gap  $\sim 0.8$  MeV. We take the  $Z = 50-82$  major shell for protons, and the  $N = 82-126$  major shell for neutrons. Although in principle we can take more than one (spherical) shell, the following conclusion is rather independent of this truncation, which makes the numerical calculation much easier. The cranked term, which is used very often for high-spin states, is not relevant because of  $\omega \approx 0$  in and near the ground state.

The feature we focus on is the matrix element of the operator

$$F_{\pi\nu} = (\mathbf{J}_\pi \cdot \mathbf{J}_\nu), \quad (3)$$

where the centered dot denotes a scalar product, and  $\mathbf{J}_\pi$  and  $\mathbf{J}_\nu$  are axial vectors denoting the proton and neutron angular momentum operators, respectively ( $\mathbf{J} = \mathbf{J}_\pi + \mathbf{J}_\nu$ ). We discuss here how  $\mathbf{J}_\pi$  and  $\mathbf{J}_\nu$  are coupled to  $\mathbf{J}$  in the present cases. The proton intrinsic state has axial sym-

metry with  $K^P=0^+$ . Therefore, for the  $z$  axis being the symmetry axis,  $|\Phi_\pi\rangle$  can be expanded into components with good angular momenta as

$$|\Phi_\pi\rangle = \sum_{J_\pi} C_\pi(J_\pi) |J_\pi, M_\pi=0\rangle, \quad (4)$$

where  $C_\pi$  indicates amplitude as a function of  $J_\pi$ ;  $|J_\pi, M_\pi\rangle$  is the component projected onto the angular momentum  $J_\pi$  and its  $z$  component  $M_\pi$ . Note that  $M_\pi=0$  due to  $K^P=0^+$ . In the present study, a state  $|J_\pi, M_\pi \neq 0\rangle$  is generated by an appropriate rotational unitary transformation from  $|J_\pi, M_\pi=0\rangle$ . The set of all the states  $|J_\pi, M_\pi\rangle$  thus constructed provides us with the complete basis for the present study. Because of its construction, the state  $|J_\pi, M_\pi\rangle$  implies the rotating state of the proton ellipsoid at an angular momentum  $J_\pi$ , and the proton angular momentum  $J_\pi$  refers hereafter to the rotation of the proton ellipsoid. The same argument is applied to neutrons; the neutron angular momentum  $J_\nu$  refers to the rotation of the neutron ellipsoid. The total intrinsic state  $|\Psi\rangle$  can be expressed as a linear combination of components with good angular momenta:

$$|\Psi\rangle = |\Phi_\pi\rangle |\Phi_\nu\rangle = \sum_J \alpha_J |\Psi_J\rangle, \quad (5)$$

with

$$|\Psi_J\rangle \equiv \sum_{J_\pi, J_\nu} \frac{1}{\alpha_J} C_\pi(J_\pi) C_\nu(J_\nu) \times (J_\pi, 0, J_\nu, 0 | J, 0) [ |J_\pi\rangle |J_\nu\rangle ]_0^{(J)}, \quad (6)$$

where  $(J_\pi, 0, J_\nu, 0 | J, 0)$  denotes a Clebsch-Gordan coefficient,  $[ |J_\pi\rangle |J_\nu\rangle ]_M^{(J)}$  implies the angular momentum coupling to  $J$  and its  $z$  component  $M$ , and  $\alpha_J \equiv [\sum_{J_\pi, J_\nu} \{ C_\pi(J_\pi) C_\nu(J_\nu) (J_\pi, 0, J_\nu, 0 | J, 0) \}^2]^{1/2}$ . The state  $|\Psi_J\rangle$  is nothing but the normalized angular-momentum-projected state from  $|\Psi\rangle$ , and includes various combinations of  $|J_\pi\rangle$  and  $|J_\nu\rangle$  in general. On the other hand, for a given  $J_\pi$  ( $J_\nu$ ), there is just one basis,  $|J_\pi\rangle$  ( $|J_\nu\rangle$ ), which is a state of the rotating ellipsoid. Note that, although Eqs. (5) and (6) are useful for gaining insight, the actual projection calculations are carried out directly on  $|\Psi\rangle$  without using  $|J_\pi\rangle$  or  $|J_\nu\rangle$ .

Figure 1(a) shows the expectation value of  $F_{\pi\nu}$  for  $J=0-24$  in the ground-state band of  $^{156}\text{Sm}$ . We point out that  $F_{\pi\nu}$  takes negative values for  $J=0-6$  in Fig. 1(a). The negative values mean that  $J_\pi$  and  $J_\nu$  point to different directions with an opening angle greater than  $90^\circ$ . In other words, contrary to the familiar picture that the proton ellipsoid and the neutron ellipsoid rotate together, these ellipsoids rotate about significantly different axes in such low-spin states. In order to see the physical meaning of this tendency, we calculate the angle  $\theta$  defined by

$$\cos\theta = \frac{\langle \mathbf{J}_\pi \cdot \mathbf{J}_\nu \rangle}{[\langle \mathbf{J}_\pi \cdot \mathbf{J}_\pi \rangle \langle \mathbf{J}_\nu \cdot \mathbf{J}_\nu \rangle]^{1/2}}, \quad (7)$$

where the angular brackets denote the expectation value

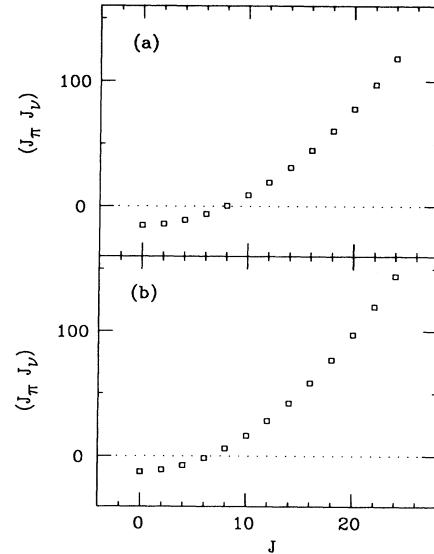


FIG. 1. Scalar product of the proton and neutron angular momentum operators for  $^{156}\text{Sm}$ . The wave functions are obtained (a) by the angular momentum projection of the Nilsson wave function and (b) by the SU(3) limit of the IBM-2.

with respect to the ground-band state with the total angular momentum  $J$ . The implication of the angle  $\theta$  is clear: It is the angle between the axial vectors  $J_\pi$  and  $J_\nu$ . If the angle  $\theta$  is near  $180^\circ$ , the proton ellipsoid and the neutron ellipsoid rotate in almost opposite ways. This is the case here, and it is schematically illustrated for the ground state in Fig. 2. Figure 3(a) presents the classical picture of the axial vectors  $J_\pi$  and  $J_\nu$  for several states in the ground-state band of the present case. In Fig. 3(a), the magnitudes of  $J_\pi$  and  $J_\nu$  are represented, respectively, by  $\sqrt{\langle \mathbf{J}_\pi \cdot \mathbf{J}_\pi \rangle}$  and  $\sqrt{\langle \mathbf{J}_\nu \cdot \mathbf{J}_\nu \rangle}$ , while their opening angle is defined by  $\theta$  in Eq. (7). It is obvious now that the angle  $\theta$  becomes smaller as the total angular momentum in-

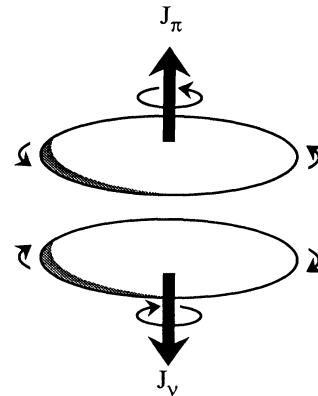


FIG. 2. Schematic picture of the rotation of the proton ellipsoid (upper) and that of the neutron ellipsoid (lower) in the ground state.

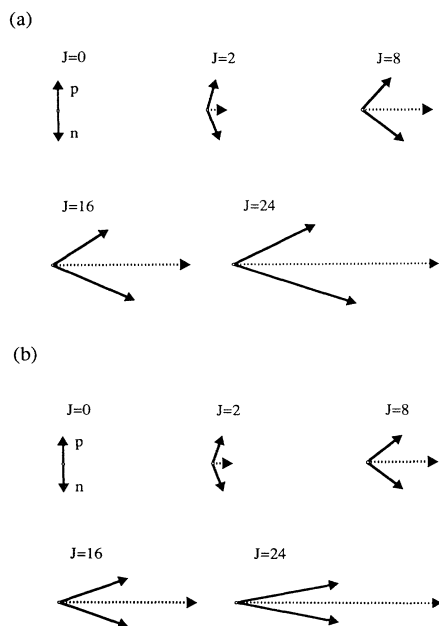


FIG. 3. Classical picture of the proton and neutron angular momenta in the ground-state rotational band of  $^{156}\text{Sm}$  (a) in the Nilsson model and (b) in the SU(3) limit of the IBM-2. Upper (lower) solid arrows denote the proton (neutron) angular momentum axial vectors. Dotted arrows are the total angular momentum vectors.

creases. In the lowest states of  $J \approx 0$ ,  $\mathbf{J}_\pi$  and  $\mathbf{J}_\nu$  are of sizable magnitude and point in almost opposite directions, and, in high angular momentum states,  $\mathbf{J}_\pi$  and  $\mathbf{J}_\nu$  are aligned in nearly the same direction. In other words, in the lowest states, the proton ellipsoid and the neutron ellipsoid rotate inversely so as to yield a nearly vanishing total angular momentum, while these two ellipsoids rotate in almost the same way in higher spin states. The latter is very close to the conventional picture of the nuclear rotation, whereas the former appears to be rather novel. Although  $\mathbf{J}_\pi$  and  $\mathbf{J}_\nu$  fluctuate in quantum mechanics, their average correlation can still be evaluated by  $\mathbf{J}_\pi \cdot \mathbf{J}_\nu$ , and is interpreted in terms of  $\theta$  in Eq. (7).

We comment on how  $|J_\pi\rangle$  and  $|J_\nu\rangle$  distribute in Eq. (6). In the case of  $J=0$  for the above example the squared amplitudes in  $|\Psi_J\rangle$  are 13%, 43%, 30%, and 11%, for  $J_\pi=J_\nu=0, 2, 4,$  and  $6$ , respectively. One might expect that only the  $J_\pi=J_\nu=0$  component has a large probability and the other components are included as a consequence of fluctuation. This is not the case; the above result shows that the probability is concentrated into  $J_\pi=J_\nu=2$  and  $4$ , whereas the probability of  $J_\pi=J_\nu=0$  is rather small. The probability distribution is shifted further away from  $J_\pi=J_\nu=0$  for stronger deformation.

The above results are obtained by variation before projection. Since the deformation is strong enough, this is a good approximation. However, in order to confirm the present consequences without such an approximation,

shell-model calculations for  $s$ - $d$  shell nuclei,  $^{20}\text{Ne}$ ,  $^{24}\text{Mg}$ , etc., have been carried out [8]. Several standard two-body interactions with short-range character are used. The results are essentially the same as those presented above.

We shall study the same problem in the IBM. Among its three symmetry limits, the SU(3) limit is suitable for the rotational motion. In this limit, the intrinsic state can be introduced, and its relation to the intrinsic state of the geometrical description has been discussed [9–11]. However, the laboratory-frame picture of the rotational states has never been discussed for the IBM either.

The ground band of the IBM-2 system with  $N_\pi=N_\nu=6$  in the SU(3) limit is taken as an example with  $N_\pi(N_\nu)$  being the number of proton (neutron) bosons. This corresponds to the  $^{156}\text{Sm}$  discussed above. We calculate matrix elements of the operator

$$F_{\pi\nu}^B = (\mathbf{J}_\pi^B \cdot \mathbf{J}_\nu^B), \quad (8)$$

where  $\mathbf{J}_\pi^B$  and  $\mathbf{J}_\nu^B$  are axial vectors denoting the proton-boson and neutron-boson angular momentum operators, respectively. The superscript  $B$  is introduced so as to distinguish from fermions (nucleons). The calculation is made for the exact eigenstates of the SU(3) Hamiltonian in the laboratory frame, while the technique in Eq. (2) for the SU(3) intrinsic state yields the identical result. In the present study, boson counterparts of the  $|J_\pi\rangle$ 's in Eq. (4) are the ground-band members of the proton-boson SU(3) system, i.e., the  $(\lambda, \mu) = (2N_\pi, 0)$  representations, and therefore mean the rotating state of the proton ellipsoid. Thus,  $\mathbf{J}_\pi^B$  represents the rotation of the proton ellipsoid about an axis perpendicular to the symmetry axis of this ellipsoid. The same argument holds for neutron bosons. Figure 1(b) presents the expectation value of  $F_{\pi\nu}^B$  in Eq. (8) for all the ground-band states. In the usual view based on the  $F$ -spin symmetry, it has been believed without an explicit reason that, in low-lying states, the proton ellipsoid and the neutron ellipsoid rotate together but very slowly. In this view, the expectation value of  $F_{\pi\nu}^B$  should be a small positive number. Note that the present IBM-2 states are totally symmetric in  $F$  spin [4,6,12]. The most striking feature in Fig. 1(b) is that the expectation value of  $F_{\pi\nu}^B$  in Eq. (8) is negative for the states of  $J=0-6$  and not necessarily small near the ground state. We calculate the angle  $\theta$ , defined similarly to Eq. (7), to clarify the physical meaning of this result. The intuitive picture of  $\mathbf{J}_\pi^B$  and  $\mathbf{J}_\nu^B$  is presented in Fig. 3(b) in a similar manner to Fig. 3(a). The nearly identical result to Fig. 3(a) is obtained, and the same physical picture holds as the one obtained for the Nilsson wave function.

We now discuss the common features obtained so far. In the ground-state rotational band, the proton ellipsoid and neutron ellipsoid rotate almost inversely in and near the ground state. In moving to higher spin states, the ellipsoid rotation axes become more aligned. The total angular momentum of the low-spin states is formed by the tilting of the proton ellipsoid rotation axis towards the

neutron one. Thus, the inverse rotation between the proton and neutron ellipsoids and the tilting of their axes characterize the rotation at lower rotational frequencies. Because of the quadrupole deformation, the density localization in a small azimuthal area around the symmetry axis occurs in the intrinsic states. Since  $\langle J_\pi^2 \rangle$  and  $\langle J_\nu^2 \rangle$  are related to this localization through the uncertainty principle, there is no way to make these quantities small in deformed states. We also mention that the present inverse rotation picture is consistent with the absence of the ground-state rotational band in single-closed nuclei, where the inverse rotation is not present due to a missing partner within the valence space. Finally, we remark that Figs. 2 and 3 are highly intuitive; although  $\mathbf{J}_\pi$  and  $\mathbf{J}_\nu$  are in a plane in those figures, they can be on different planes, because various magnetic substates contribute with the weights given by Clebsch-Gordan coefficients so as to form a total angular momentum. This does not change the results of the present study, because their correlation [i.e., the scalar products in Eqs. (4) and (8)] should remain as discussed above.

After having obtained the picture of the nuclear rotation in the laboratory frame, we should address the question of the energy of the rotational states. In the ground state, the wave functions of the rotating proton and neutron ellipsoids have the precisely opposite axes, and hence the wave function of the rotating proton ellipsoid and that of the rotating neutron ellipsoid have maximum spatial overlap. This situation is similar to the pairing interaction. In the  $2^+$  state,  $\mathbf{J}_\pi$  is not completely opposite to  $\mathbf{J}_\nu$ . Thus,  $\mathbf{J}_\pi$  is tilted somewhat towards  $\mathbf{J}_\nu$ . We now introduce the proton (neutron) rotation disk representing the average distribution of the rotating proton (neutron) ellipsoid. The proton rotation disk and the neutron rotation disk are completely identical in the ground state because  $\mathbf{J}_\pi$  and  $\mathbf{J}_\nu$  are completely opposite. In the  $2^+$  state, the proton rotation disk is also tilted due to the tilting of its axis, and the wave function of the rotating proton ellipsoid has a somewhat smaller overlap with that of the neutrons in comparison to this overlap for the ground state. The smaller overlap means in general a smaller gain in the binding energy. Thus, by tilting  $\mathbf{J}_\pi$  towards  $\mathbf{J}_\nu$  (or vice versa), the total system loses some attractive energy, and this energy loss results in the rotational energy, for lowest angular momentum states. In other words, the moment of inertia can be considered partly as the inertial parameter against the tilting of the proton and neutron rotation axes. Note that the  $J=0$  state is formed by a superposition of various components  $|J_\pi=L, M_\pi=M\rangle|J_\nu=L, M_\nu=-M\rangle$ , and therefore gains a sizable energy from off-diagonal matrix elements among them. In fact, the proton-neutron quadrupole interaction produces such matrix elements. A similar mechanism is present for low-lying states, whereas high-spin states can obtain less energy due to more limited configurations.

It is worthwhile to mention the cranking calculation of the moment of inertia. Since the change in tilting angle

for  $\Delta J=2$  is rather small, the structure change between them is small, and the effect may be treated in a perturbative way, i.e., the Inglis formula [13].

Another aspect to be mentioned is the net matter flow. For  $2^+$ , for instance, if one sees the nucleus from the direction of the total angular momentum (from the right in Fig. 3), the rotation of the proton ellipsoid is not completely canceled by the rotation of the neutron ellipsoid for the motion projected onto the plane perpendicular to the total angular momentum vector  $\mathbf{J}$ . This remaining flow corresponds to the slow rotation in the classical picture.

The inverse rotation produces a finite value of  $\langle 0^+ | (\mathbf{J}_\pi - \mathbf{J}_\nu)^2 | 0^+ \rangle$ , which is related to the scissors-mode  $M1$  sum rule [12,14]. Observed values of this sum rule in deformed nuclei [14] provide experimental support.

In the present study, the total angular momentum is divided into  $\mathbf{J}_\pi$  and  $\mathbf{J}_\nu$  based on the property of the deformed mean field. In other quantal systems, however, different divisions may be taken; for instance, in  $^8\text{Be}$ , the division into two  $\alpha$  clusters will be more appropriate.

The author acknowledges Professor A. Gelberg for a careful reading of the manuscript and Professor A. Arima for useful discussions. The author is grateful to the participants of the program 9 at the Institute for Nuclear Theory in Seattle, in particular Professor I. Talmi, for their useful discussions. This work has been supported in part by the Grant-in-Aid for General Scientific Research (No. 01540231) by the Ministry of Education, Science, and Culture. The numerical calculations have been carried out at the Computer Centre and at the Meson Science Laboratory in the University of Tokyo.

- [1] S. G. Nilsson, *Mat. Fys. Medd. Dan. Vidensk. Selsk.* **29**, No. 16 (1955); S. G. Nilsson and O. Prier, *Mat. Fys. Medd. Dans. Vidensk. Selsk.* **32**, No. 16 (1961).
- [2] A. Bohr and B. R. Mottelson, *Nuclear Structure* (Benjamin, New York, 1975), Vol. 2.
- [3] F. Iachello and A. Arima, *The Interacting Boson Model* (Cambridge Univ. Press, New York, 1987).
- [4] A. Arima, T. Otsuka, F. Iachello, and I. Talmi, *Phys. Lett.* **66B**, 205 (1977).
- [5] T. Otsuka, A. Arima, F. Iachello, and I. Talmi, *Phys. Lett.* **76B**, 139 (1978).
- [6] T. Otsuka, A. Arima, and F. Iachello, *Nucl. Phys.* **A309**, 1 (1978).
- [7] J. L. Egido and P. Ring, *Nucl. Phys.* **A383**, 189 (1982).
- [8] T. Otsuka and M. Honma (to be published).
- [9] J. N. Ginocchio and M. W. Kirson, *Nucl. Phys.* **A350**, 31 (1980).
- [10] A. E. L. Dieperink, O. Scholten, and F. Iachello, *Phys. Rev. Lett.* **44**, 1747 (1980).
- [11] A. Bohr and B. R. Mottelson, *Phys. Scr.* **22**, 468 (1980).
- [12] T. Otsuka, in *Algebraic Approaches to Nuclear Structure: Interacting Boson and Fermion Models*, edited by R. F. Casten (Harwood Academic, Langhorne, 1993), Chap. 4.
- [13] D. R. Inglis, *Phys. Rev.* **96**, 1059 (1954).
- [14] A. Richter, *Nucl. Phys.* **A522**, 139c (1991).